Sources of Instabilities in Two-Way Satellite Time Transfer

T.E. Parker and V. Zhang
National Institute of Standards and Technology
Time and Frequency Division
325 Broadway
Boulder, CO USA

Abstract -- **Two-Way Satellite Time and Frequency Transfer (TWSTFT) has become an important component in the international system for comparing time and frequency over long distances. In order to make further improvements in the stability of TWSTFT a more complete understanding of the sources of instabilities is required. This paper analyzes several sources of instabilities, including environmental factors, ionospheric delay, satellite motion and the satellite transponder.**

I. INTRODUCTION

Two-Way Satellite Time and Frequency Transfer (TWSTFT) regularly delivers subnanosecond time transfer stability at 1 day as measured by the time deviation (TDEV) statistic. Occasionally 1 day stabilities at, or below, 100 ps are now being observed [1], (also see Section IV). As a result TWSTFT has become an important component in the international system for comparing time and frequency over long distances.

In order to obtain improvements in the stability (precision) of two-way satellite time and frequency transfer the sources of the time delay instabilities must be understood and reduced. Kirchner [2] has discussed many of these sources but a more detailed investigation is now needed as TWSTFT stability continues to improve. To obtain further improvements it is necessary to evaluate all potential sources of time transfer instability, and to reduce or eliminate them. The Time and Frequency Division of the National Institute of Standards and Technology (NIST) has had a long standing project to address this goal. The objective is to eventually achieve a stability of 10 ps as measured by TDEV at a one day averaging time for long-baseline TWSTFT. As part of this project we have been evaluating the environmental sensitivities of a number of microwave components and systems. In particular we have measured sensitivities to temperature and relative humidity in Ku-band amplifiers, filters, up-converters and down-converters. Temperature sensitivities vary significantly among different pieces of equipment, but can be as small as a few ps/C. We have observed sensitivity to relative humidity at the 1 ps/% level. We have also measured the temperature sensitivity for several earth station systems. Calculated time deviation, TDEV, plots of time transfer instability due to temperature fluctuations based on measured temperature sensitivity and outside temperatures for a period of nearly 2 years are shown. TDEV characteristics for relative humidity and barometric pressure are also presented. Using the International GPS Service (IGS) ionosphere maps we have also investigated the level of instability in Ku-band TWSTFT caused by variations in the ionosphere and TDEV plots are shown. The communication satellite itself can cause instabilities through its motion, and from delay instabilities in the transponder. These are discussed along with other potential sources of instability.

Caution must be exercised in the use of TDEV as a measure of time transfer stability. The magnitude of TDEV is sensitive to the density of data (number of data points per day) even for flicker PM noise. This makes the comparison of different time transfer techniques more complicated than it might appear. This is discussed and an example will be shown.

II. ENVIRONMENTAL SENSITIVITIES

Almost no information is available from manufacturers on the sensitivity of group delay to environmental parameters for the equipment used in TWSTFT. As a result we have measured these sensitivities on equipment as we have had access to it. The data presented here are not intended to be a comprehensive survey, but simply to give an idea of the magnitudes that are present. Table 1 below shows the values (or range of values) and uncertainties for the temperature coefficients of group delay observed on a variety of modules used in typical TWSTFT systems, including low noise amplifiers (LNA's), high power amplifiers, filters, mixers, isolators, up- and down-converters and two-way modems. Most measurements were made over the range of 5 to 45 C at a constant relative humidity of 40 %. In this and other tables the path stated in the comments column indicates whether the delay is for the individual transmit (Tx) or receive (Rx) paths, or for the combined transmit and received paths, ((Tx-Rx)/2)), as

0-7803-9052-0/05/$20.00 © 2005 IEEE.

appear in the two-way equations [2]. Uncertainties in the measurements are indicated in parentheses.

TABLE 1 Temperature Coefficients of Group Delay (+5 to +45 C at 40 % relative humidity)

Modules

Equipment	Temp. Co. (ps/C)	Comments
High Power Amplifier	-5 (±2)	Tx path
LNAs and filters	-5 to +2 (±2)	Rx path
Mixer plus two isolators	-18 (±2)	Tx or Rx path
Up-Converters	-4 to +1 (±2)	Tx path
Down-Converters	+2 to +10 (±2)	Rx path
Modem	-20 (±2)	Tx+Rx path

Table 2 shows measured temperature coefficients of group delay for several different sets of equipment that are usually situated outside in a location that is near the dish antenna. This equipment consists of up and down-converters, and usually also contains the high power amplifier, LNA and filters. Equipment shown in Table 2 as being in the "box" is similar to that in the hub except it is usually packaged as a unit for physically small systems. References are shown in brackets in the table.

TABLE 2 Temperature Coefficients of Group Delay (nominally 0 to +50 C)

Systems

Equipment	Temp. Co. (ps/C)	Comments
All equip. in hub (sys. A)	+5 (±5)	(Tx-Rx)/2
All equip. in hub (sys. B) [3]	+50 (±10)	(Tx-Rx)/2
All equip. in box (sys. C) [3]	-180 (±50)	(Tx-Rx)/2
All equip. in box (sys. D) [4]	+10 (±5)	(Tx-Rx)/2

The equipment in system A in Table 2 is predominantly made up of modules measured in Table 1. The other systems are all older systems for which no data is available on individual modules. Note that reflections in transmission lines may cause the temperature coefficient of a system to be different from the sum of its parts [5].

Table 3 shows sensitivities to relative humidity (RH) for several different modules measured over the nominal range of 20 to 60 % RH at 25 C. No data is available on the sensitivity to relative humidity for systems.

TABLE 3 Sensitivity to Relative Humidity (20 to 60 % at 25 C)

Modules

Equipment	Coefficient (ps/%)	Comments
LNA and filter	-0.3 (±0.1)	Rx path
Up-Converters	0.4 to 1 (±0.1)	Tx path
Down-Converter	0.8 (±0.1)	Rx path

Figures 1 to 4 show calculated TDEV levels for several environmental parameters measured at the NIST facility in Boulder using reasonable values for environmental sensitivities. In all plots there are 12 equally spaced measurements per day for the relevant environmental parameters (temperature, relative humidity and barometric

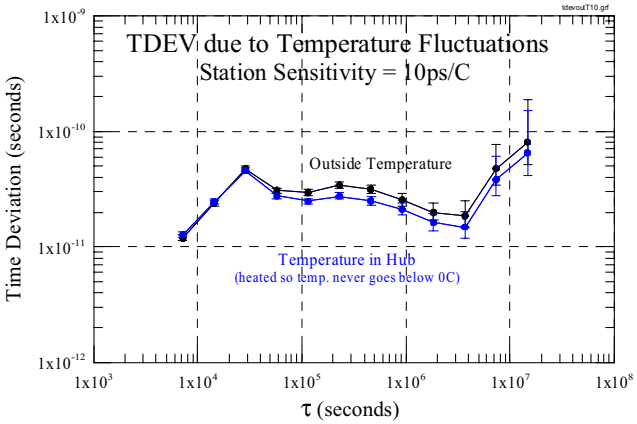

Figure 1. Calculated TDEV for a station sensitivity of 10 ps/°C. This is the contribution from one station, using the outside temperature at Boulder, CO USA (upper curve). The earth station hub has a heater in it that prevents the temperature in the hub from going below 0 °C (lower curve).

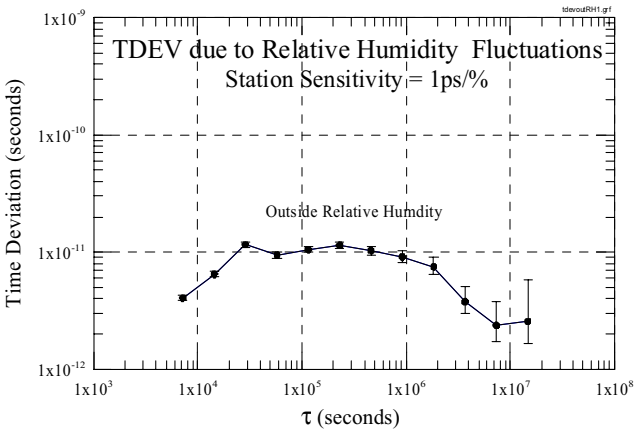

Figure 2. Calculated TDEV for a sensitivity of 1 ps/%. This is the contribution from one station, using the outside relative humidity at Boulder, CO USA.

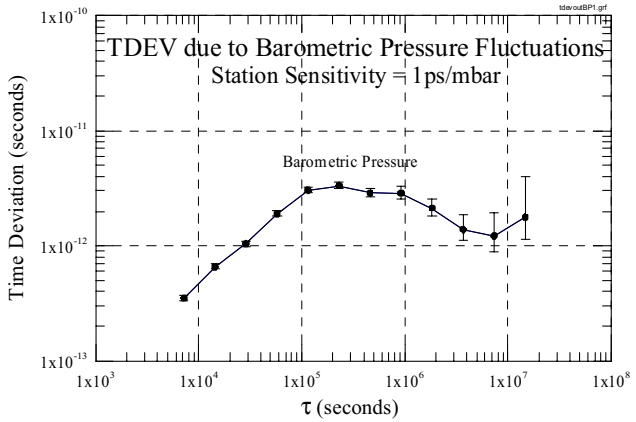

Figure 3. Calculated TDEV for a sensitivity of 1 ps/mbar. This is the contribution from one station, using the barometric pressure at Boulder, CO USA.

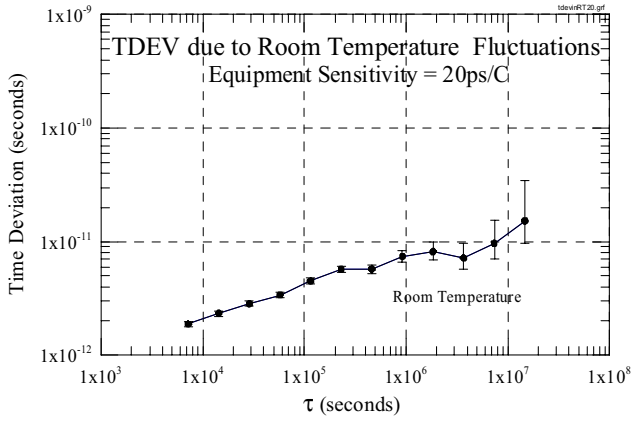

Figure 4. Calculated TDEV for a sensitivity of 20 ps/°C. This is the contribution from one station, using the room temperature at the NIST two-way room in Boulder, CO USA.

pressure).

Figure 1 shows the TDEV for a station sensitivity of 10 ps/C. This is the contribution from one station, using the outside temperature at Boulder, CO USA (upper curve) over a period of nearly two years. The earth station hub has a heater in it that prevents the temperature in the hub from going below 0 C and the TDEV using this temperature data is shown in the lower curve. Note the roughly flicker phase nature of the TDEV. Figure 2 shows the calculated TDEV for relative humidity using a sensitivity of 1 ps/%. This is again the contribution from one station and using the outside RH at NIST in Boulder. (Note that the RH in Boulder varies from 0 to 100%, which is a relatively large swing.) Figure 3 shows the calculated TDEV for barometric pressure using a sensitivity of 1 ps/mbar. This is the contribution from one station, using the barometric pressure at NIST in Boulder. Though the sensitivity to barometric pressure has not been measured, this graph is presented to show the shape of the TDEV curve. Figure 4 shows the calculated TDEV for indoor temperature and a sensitivity of 20 ps/C. This is the contribution from one station using the room temperature (rather poorly controlled at ± 4 C) in the NIST two-way room in Boulder. Note that all the TDEV values will scale linearly with any of the environmental sensitivities.

Obviously the equipment located outside is going to be subjected to larger swings in temperature and humidity and therefore needs to be chosen for minimum sensitivity. In addition some level of environmental control on outside equipment may also be required, including the possibility of humidity control. Indoor equipment may not need environmental control if the sensitivities are sufficiently small. However, indoor humidity control may be required for TDEV stabilities below 10 ps.

TDEV plots for time transfer instabilities quite often exhibit a flicker phase modulation (FPM) characteristic, and this is most similar to that reflected in Fig. 1, indicating that outdoor temperatures are most likely a major cause of TWSTFT instabilities, though relative humidity may also be a contributor. Evidence of daily, multiday, and annual temperature cycles is present in Fig. 1.

III. IONOSPHERIC DELAY

The ionospheric delay in the TWSTFT measurements made by one two-way station can be shown by the equation below.

$$d_{ION} = \frac{1}{2} \cdot \frac{40.3}{c} \cdot TEC \cdot \left(\frac{1}{f_{TX}^2} - \frac{1}{f_{RX}^2} \right), \quad (1)$$

where c is the speed of light in vacuum (constant), TEC is the total electron content integrated over the path through the ionosphere, and f_{TX} and f_{RX} are the two-way station's transmit and receive frequencies.

Because the TEC varies with solar activity, the daytime TEC is higher than the nighttime TEC. The TEC also varies day by day and annually (small in winter, large in summer). Different locations are likely to have different TEC values, and therefore will have different ionospheric delays in the TWSTFT signals. For a given time and location, the ionospheric delay of the TWSTFT signal is also a function of the elevation angle of the satellite relative to the two-way station. The lower the elevation angle, the longer the TWSTFT signal has to travel through the ionosphere (larger TEC) and the larger the ionospheric delay introduced into the measurements will be. The two TWSTFT stations may also use different sets of transmit and receive frequencies due to the satellite transponder configuration. Therefore, the ionospheric delay in the two sets of measurements will not be completely cancelled in the TWSTFT difference.

To study the instability introduced by the ionospheric delay, we evaluated the ionospheric delay with the global TEC map provided by the IGS. The TEC map is contained

in the daily IONosphere map EXchange format (IONEX) file. In the IONEX files, the TEC values are reported at a 2-hour epoch with a 2.5 degree latitude by 5 degree longitude grid on a sphere 450 km above the earth's surface. To obtain the ionospheric delay for the TWSTFT measurement at a given two-way station at a given time, we use the nominal coordinates of the satellite and the coordinates for the earth station to determine the TWSTFT signal's penetration point on the TEC map at the given time. With the TEC value, we then use the transmit and receive frequencies to obtain the ionospheric delay. The estimated hourly ionospheric delays for the TWSTFT links between NIST and the Physikalisch-Technische Bundesanstalt (PTB) in Germany and between NIST and the U.S. Naval Observatory (USNO) in Washington DC are shown in Figs. 5 and 6. The horizontal axis of both figures is the Modified Julian Day (MJD).

In both figures, we see that the ionospheric delay at one

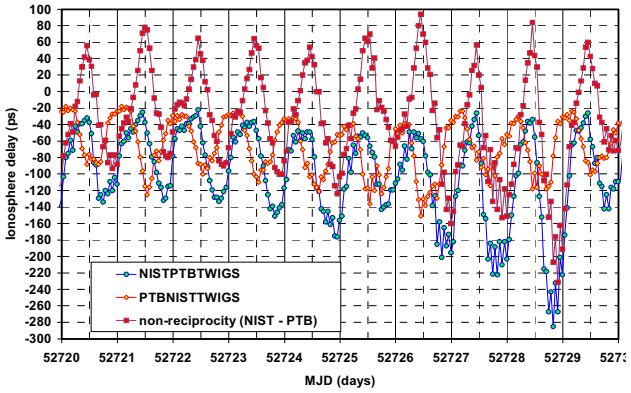

Figure 5. Ionospheric delay and the non-reciprocity for the NIST/PTB link (Satellite E 325.5°, elv_{NIST} = 6°, elv_{PTB} = 17°, f_{TX} = 14.34 GHz, f_{RX} = 11.54 GHz).

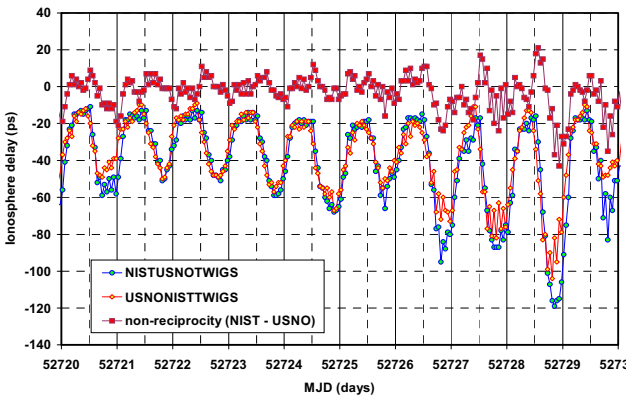

Figure 6. Ionospheric delay and the non-reciprocity for the NIST/USNO link (Satellite E 273°, elv_{NIST} = 40°, elv_{USNO} = 44°, f_{TX} = 14.43 GHz, f_{RX} = 12.13 GHz).

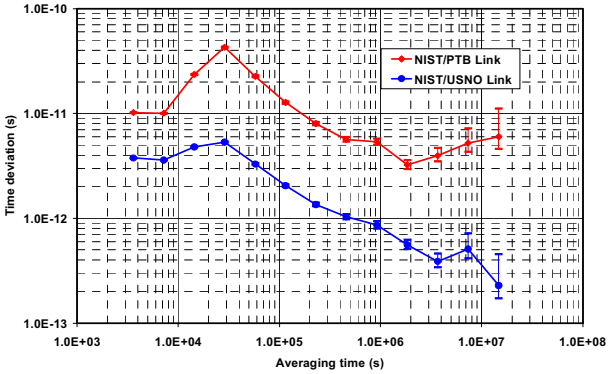

Figure 7. TDEV for the non-reciprocity due to the ionospheric delay.

two-way station has a negative mean. This is due to the fact that the receive frequency is lower than the transmit frequency. So, the received TWSTFT signal suffers more ionospheric delay than the transmited signal. We also see that the ionospheric delay has a diurnal structure. The delay gets more negative during the daytime. In Fig. 5, we see that the ionospheric delay at NIST has a larger peak to peak variation then that at PTB. This is caused by the lower elevation angle of the NIST two-way station antenna. In Fig. 5, we also see that the diurnal structure of the NIST ionosphere delay is shifted to the right of that for PTB, because a new day at PTB starts 7 hours earlier than at NIST in Boulder, Colorado. Figures 5 and 6 also contain the difference of the ionospheric delays of the TWSTFT links which shows the path delay non-reciprocity introduced by the ionospheric delay. The difference of the ionospheric delay for the NIST/PTB link reaches a peak of hundreds of picoseconds with a diurnal structure and a nonzero mean. The time zone difference and the low elevation angle at NIST are the major contributors to the result. Most of the ionospheric delay in the NIST/USNO link is canceled in the difference, because of the short baseline between the two stations, only a 2-hour time zone difference, and similar elevation angles to the satellite. Although small, the non-reciprocity is still in the tens of picoseconds range, which should be taken into consideration if one wants to achieve the best stability. The time deviations of the non-reciprocity due to the ionospheric delay for the NIST/PTB and the NIST/USNO links are shown in Fig. 7.

It should be pointed out that the ionospheric delay obtained with the IGS TEC map contains errors caused by the relatively coarse density of the epoch and grid. Also, some parts of the earth may not have a good TEC map. The error in the estimate would also increase for a low elevation angle between the two-way station and the satellite.

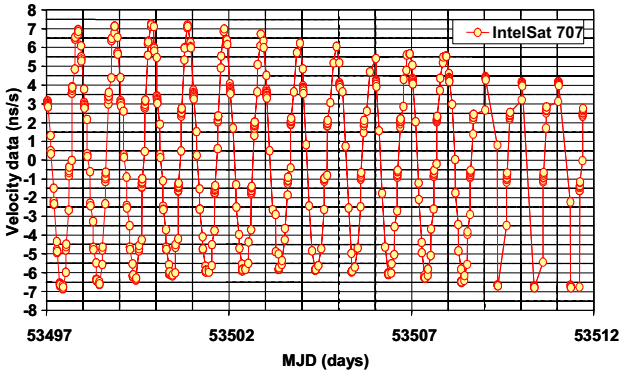

Figure 8. Velocity of satellite at 307E as measured at NIST during the transatlantic TWSTFT sessions.

IV. SATELLITE MOTION

A geostationary satellite has a daily motion relative to the earth's surface. As a result, the TWSTFT path length (station A → satellite → station B, and vice versa) varies in a sinusoidal pattern everyday. Figure 8 shows the velocity in ns/s (path delay change) of the satellite at 307E as measured at NIST during the transatlantic TWSTFT sessions. In general, the distance of station A to the satellite and the distance of station B to the satellite are not exactly symmetrical. For example, with Intelsat 707 at 307E the signal from NIST will arrive at the satellite about 2.0 ms before the signal from the National Physical Laboratory (NPL) of the United Kingdom. For the NIST/PTB link the NIST signal arrives about 4.3 ms earlier. With a positive satellite velocity, the signal that arrives later at the satellite will have a longer path than the signal that arrives earlier. Therefore, the path delays won't be completely canceled in the TWSTFT difference. Because of the satellite motion, the path non-reciprocity introduces instability in the TWSTFT results.

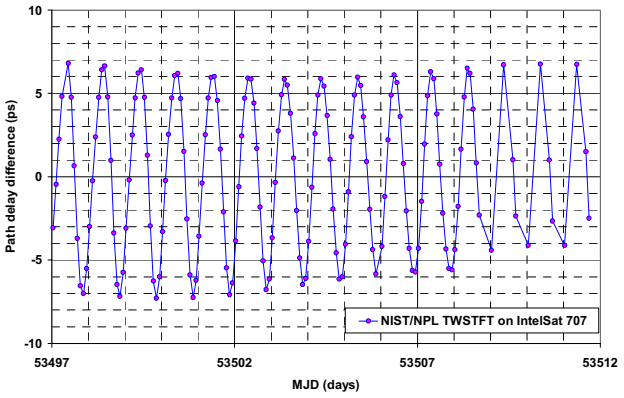

Figure 9. Path delay difference for the NIST/NPL link based on the velocity measured at NIST. For the NIST/PTB link it is two times larger.

Assuming that the path delay change shown in Fig. 8 is caused mostly by the radial satellite motion, we estimate the path non-reciprocity for the NIST/NPL link by multiplying half the velocity of Fig. 8 by the fractional delay per second (for example 2 x 10^{-3}/1 for NIST/NPL). The result is shown in Fig. 9. An error of about ± 7 ps is introduced into the NIST/NPL link by the satellite motion. For NIST/PTB it would be more than twice as large. From Fig. 9, we notice that the mean of the daily averaged path non-reciprocity is very close to zero when TWSTFT was performed with 12 equally spaced sessions. On the other hand, the mean of the daily averaged path non-reciprocity is slightly larger than zero when TWSTFT was performed at 0:00, 8:00, 14:00 and 16:00 UTC (last four days in Figs. 8 and 9). This shows that the impact of the path non-reciprocity on a daily average due to the satellite motion can be minimized by doing TWSTFT with the sessions distributed symmetrically about the sinusoidal pattern.

V. SATELLITE TRANSPONDER INSTABILITY

This can be a problem when the two path directions don't go through the same transponder, as on the transatlantic links. On MJD 53206 a 5 ns time step was observed in UTC(NIST) – UTC(PTB) as shown in Fig. 10, when nothing on the ground had changed. Other transatlantic links observed similar time steps. This was most likely caused by interference and increased traffic on the satellite transponder.

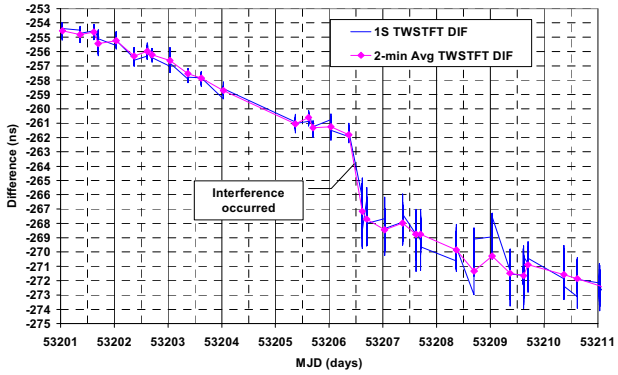

Figure 10. Time step in UTC(NIST) – UTC(PTB) TWSTFT difference due to changes on the satellite transponder (interference, load?).

As first observed by Lee Breakiron [6] of the USNO, the interference also increased the short term instability as shown in Figs. 11 and 12. Note that the slope over a typical 120 second session became more variable after the interference appeared. The stability of the transatlantic TWSTFT link improved when it was moved to a different satellite. The signal strength was about the same, but there was no other traffic to cause interference or load the

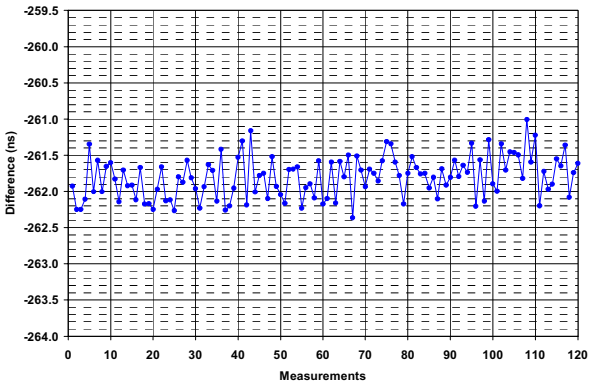

Figure 11. Typical one-second UTC(NIST) – UTC(PTB) TWSTFT difference before the satellite transponder interference

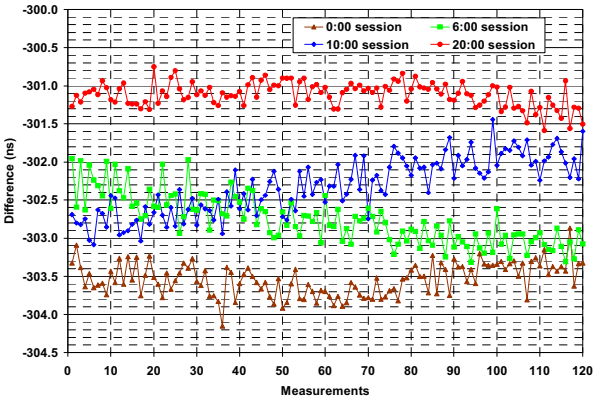

Figure 12. Instability in the one-second UTC(NIST) – UTC(PTB) TWSTFT difference (on MJD 53310) due to satellite transponder interference. Note the slope changes.

transponder on the new satellite. An immediate improvement was seen in the 4 times per day data just before and after the satellite change. However, this improvement is best illustrated with data from two sessions 150 days apart where data was collected 12 times per day as shown in Fig. 13. Unfortunately we did not have data at a rate of 12 times per day immediately prior to the satellite change.

VI. OTHER POSSIBLE SOURCES OF INSTABILITIES

In addition to the instabilities discussed above there are also other potential sources. We have seen temperature coefficients as large as 200 ps/C in 1 pulse per second (PPS) generators. This can affect the REFDELAY measurement required with many TWSTFT modems. We have also measured temperature coefficients in NIST-designed 1 PPS distribution amplifiers, and in this case the temperature coefficients were in the range of -0.6 to -3.2 ps/C. At this level this is not a problem for indoor equipment.

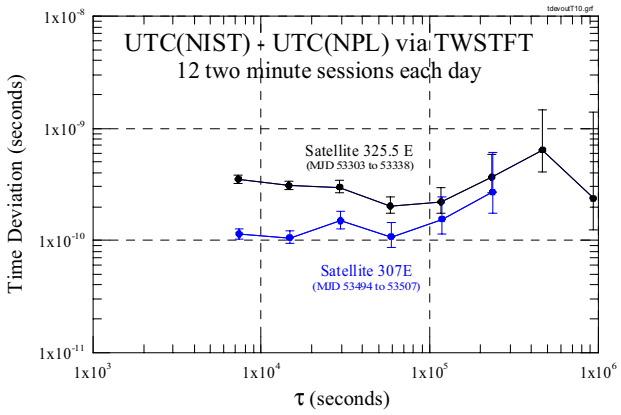

Figure 13. Improved link stability when moved to a different satellite with no interference on the transponder.

Generally the troposphere is assumed to be non-dispersive at the nanosecond level, but is it at the 10 ps level? There are microwave absorption resonances in the atmosphere, and this can lead to dispersion.

VII. CAUTION ON USING TDEV FOR COMPARING SYSTEM STABILITIES

The TDEV statistic is sensitive to the data density. This is large and well known for white PM noise but it is also true for flicker PM noise, [7] as illustrated in Fig. 14. The same data set with 12 points per day that was used to generate the black (lower) curve was thinned to only 1 point per day to generate the red (upper) curve. The lower data density gives larger TDEV values for the 3 smallest τ values. In comparing the stabilities of different time transfer systems it is important to take into account the different data densities. For example, time transfer systems based on the GPS system generally have much larger data densities than that of TWSTFT. The sensitivity to data density is significantly less for slower noise processes such

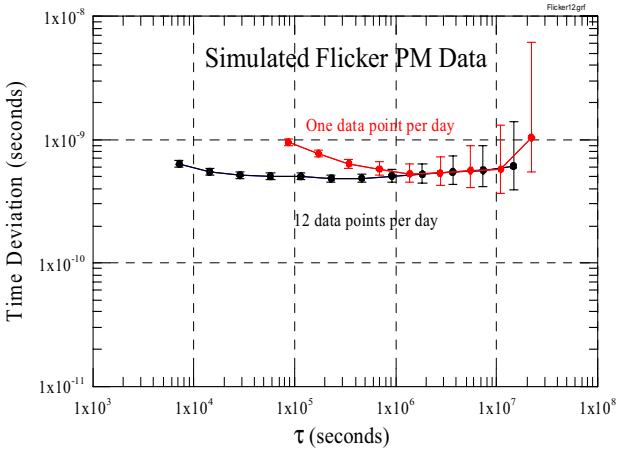

Figure 14. Simulated Flicker PM data at two different densities.

as white FM, flicker FM, or random walk FM [7].

VIII. CONCLUSIONS

Though we have quantified many sources of instabilities, it is not clear that we have identified all sources, since the observed instabilities in real two-way links are larger than expected from the known sources. However, we have not yet quantified the environmental sensitivities at both stations in a two-way link. Thus a firm estimate of the total contribution of environmental sensitivities cannot yet be made. The fact that time transfer instabilities in many two-way links appear to have TDEV characteristics that are consistent with flicker PM noise (see Fig. 13) would seem to indicate that environmental parameters such as temperature and possibly humidity are a major source of instabilities. We saw in Fig. 1 that outside temperature gave a roughly flicker PM characteristic. When you consider that over long baselines the diurnal cycles will be out of phase and multi-day weather cycles will not occur at the same time, it is not unreasonable to expect that some of the sharp peaks observed in Fig. 1 will get smeared out in a real two-way link. The data from this investigation shows that the ionosphere and satellite motion are not significant sources of two-way instability at the 100 ps TDEV level.

Some additional areas to investigate are: (1) environmental sensitivities in other parts of the system, including cables, reflections, etc. and other environmental parameters such as barometric pressure, (2) satellite transponder instabilities and, (3) influence of the troposphere.

With corrections for the ionosphere and satellite motion, higher chip rates, and control of environmental factors, a link stability of 10 ps TDEV at 1 day (12 two minute sessions per day) seems like an achievable goal. However more investigation is needed. Instabilities in the satellite transponder could be a serious problem for certain links since they are out of the user's control.

ACKNOWLEDGEMENT

We gratefully acknowledge Intelsat for the use of satellite time at no cost. Also, we acknowledge PTB and NPL for the use of their TWSTFT data.

REFERENCES

[1] A. Bauch, et. al., "Time and Frequency Comparisons Between Four European Timing Institutes and NIST using Multiple Techniques" to be published in the Proceedings of the 2005 European Frequency and Time Forum.

[2] D. Kirchner, "Two-Way Satellite Time and Frequency Transfer (TWSTFT): Principle, Implementation, and Current Performance," Review of Radio Science 1996-1999, Oxford University Press, New York, NY USA, pp. 27-44, 1999.

[3] Franklin G. Ascarrunz, "Timing Errors in Two-Way Satellite Time and Frequency Transfer using Spread Spectrum Modulation," Ph.D. thesis, Univ. of Colorado, 1999.

[4] Wayne Hanson, private communication.

[5] F. G. Ascarrunz, T. E. Parker and S. R. Jefferts, "Group-Delay Errors Due to Coherent Interference," in Proc. Joint Meeting of the European Frequency and Time Forum and the IEEE International Frequency Control Symposium, pp 198-202, 1999.

[6] Lee Breakiron, private communication, 2004.

[7] M. A. Weiss, F. L. Walls, C. Greenhall and T. Walter, "Confidence on the Modified Allan Variance and the Time Variance," in Proc. of the 9th European Frequency and Time Forum, pp. 153-165, 1995.